Journal Pre-proofs

Development of dissolving microneedles using a quality by design approach for transdermal delivery of the nanoemulsified volatile compound β-caryophyllene

Patrícia Weimer, Isabella Morel Bordignon, Alexandre Rolim Mineto, Karen de Oliveira Araujo, Júlia Cordeiro Waszak, Nathalya Tesch Brazil, Fabrício Mezzomo Collares, Maria Dul, Rochele Cassanta Rossi, Letícia Scherer Koester

PII: S0378-5173(26)00064-5
DOI: https://doi.org/10.1016/j.ijpharm.2026.126616
Reference: IJP 126616

To appear in: *International Journal of Pharmaceutics*

Received Date: 11 November 2025
Revised Date: 23 December 2025
Accepted Date: 21 January 2026

Please cite this article as: P. Weimer, I.M. Bordignon, A.R. Mineto, K. de Oliveira Araujo, J.C. Waszak, N.T. Brazil, F.M. Collares, M. Dul, R.C. Rossi, L.S. Koester, Development of dissolving microneedles using a quality by design approach for transdermal delivery of the nanoemulsified volatile compound β-caryophyllene, *International Journal of Pharmaceutics* (2026), doi: https://doi.org/10.1016/j.ijpharm.2026.126616

Development of dissolving microneedles using a Quality by Design approach for transdermal delivery of the nanoemulsified volatile compound β-caryophyllene

Patrícia Weimer[1]; Isabella Morel Bordignon[1]; Alexandre Rolim Mineto[1]; Karen de Oliveira Araujo[1]; Júlia Cordeiro Waszak[1]; Nathalya Tesch Brazil[1]; Fabrício Mezzomo Collares[2]; Maria Dul[3]; Rochele Cassanta Rossi[4]; Letícia Scherer Koester[1,*]

[1] Programa de Pós-Graduação em Ciências Farmacêuticas, Faculdade de Farmácia, Universidade Federal do Rio Grande do Sul (UFRGS), Av. Ipiranga, 2752, Santa Cecília, Zip code 90610-000, Porto Alegre, Rio Grande do Sul, Brazil.

[2] Laboratório de Materiais Dentários, Faculdade de Odontologia, Universidade Federal do Rio Grande do Sul (UFRGS), Rua Ramiro Barcelos, 2492, Santa Cecília, Zip code 90035-004, Porto Alegre, Rio Grande do Sul, Brazil.

[3] School of Pharmacy and Pharmaceutical Sciences, Cardiff University, Redwood Building, King Edward VII Ave, Cardiff CF10 3NB, Cardiff, UK.

[4] Programa de Pós-Graduação em Nutrição e Alimentos, Universidade do Vale do Rio dos Sinos (UNISINOS), Av. Unisinos, 950, Cristo Rei, Zip code 93022-000, São Leopoldo, Rio Grande do Sul, Brazil.

[*] **Correspondence:**

L. S. Koester. E-mail address: leticia.koester@ufrgs.br | Address: Av. Ipiranga 2752, Santa Cecília, Zip code 90610-000, Porto Alegre, Rio Grande do Sul, Brazil | Tel.: +55 51 33085278; Fax: +55 51 33085437.

ABSTRACT

This study examines transdermal delivery of a β-caryophyllene (a lipophilic and volatile compound) loaded nanoemulsion from dissolving water-soluble polymer microneedles (microneedle array patches - MAPs). Development of this system was guided by the principles of Quality by Design; after defining a quality target product profile and critical quality attributes, a rational experimental plan optimized a formulation to maximize the β-caryophyllene content in MAPs. The optimized formulation consists of polyvinyl pyrrolidone combined with polyvinyl alcohol (combination ratio of 1.54) and a β-caryophyllene-to-polymer mass ratio of 0.09. The β-caryophyllene content was maintained higher than 95% in relation to the additional mass following the micromolding process and after 45 days of storage. *In vitro* skin insertion, dissolution, mechanical properties, and transdermal delivery have been investigated for the prototype. A key feature of this work is demonstrating the feasibility of delivering a volatile compound through MAP by associating it with a nanoemulsion. This combined delivery method allows for the transdermal administration of β-caryophyllene, which cannot be achieved through topical nanoemulsion application alone. Overall, the developed system offers a promising alternative to traditional topical and oral pharmaceutical dosage forms.

Keywords: sesquiterpene; β-caryophyllene; microneedle; critical quality attributes; design space; risk management

1. INTRODUCTION

β-caryophyllene ($C_{15}H_{24}$, MW 204.36 g/mol) is a bicyclic sesquiterpene found in essential oils from various plant species, including copaiba (*Copaifera* spp.), hemp (*Cannabis sativa*), oregano (*Origanum vulgare*), and cloves (*Syzygium aromaticum*). In its isolated or synthetic form, β-caryophyllene appears as a yellowish liquid at room temperature and has a woody-spicy aroma (Gertsch et al., 2008; National Center for Biotechnology Information, 2019; Sharma et al., 2016). Beyond its fragrance, this compound has gained increasing interest because of its notable therapeutic effects, including anti-inflammatory, analgesic, immunomodulatory, antibacterial, antioxidant, and antiparasitic activities (Cheng et al., 2014; Francomano et al., 2019; Meza and Lehmann, 2018; Sharma et al., 2016).

The therapeutic effects of β-caryophyllene arise from its multi-target mechanism of action. Its anti-inflammatory activity is linked to the inhibition of enzymes such as cyclooxygenase-2, myeloperoxidase, inducible nitric oxide synthase, and NADPH oxidase, along with the modulation of pro-inflammatory mediators such as interleukins (i.e., interleukin-1, -6, -8, and -10), tumor necrosis factor-alpha, and interferon gamma. The compound's analgesic action primarily involves type 2 endocannabinoid receptors (CB2) and μ-type opioid receptors (Klauke et al., 2014; Sharma et al., 2016).

β-caryophyllene's lipophilicity (Log *P* 4.4) and volatility limit its pharmacological applications (NCBI, 2022), however formulation strategies have been developed to overcome these limitations. For example, its association with a self-emulsifying drug delivery system has demonstrated increased plasma levels compared to free β-caryophyllene following oral administration (Mödinger et al., 2022). Topical application of β-caryophyllene in nanoemulsion or nanoemulsion-thickened hydrogel formulations has also been investigated (Peterle et al., 2020; Weimer et al., 2022), however it is challenging to achieve localized therapeutic levels due to the restrictive nature of the stratum corneum. In the respective studies, in vitro permeation tests showed the deposition of β-caryophyllene in the skin layers, with saturation in the dermis when delivered in nanoemulsion. The compound was not measured in the receptor fluid, even under damaged skin conditions. Therefore, it is necessary to explore other technologies that facilitate the transdermal delivery of this compound.

Microneedle array patches (MAPs) provide a potential method to enhance skin permeation (Dul et al., 2025; Moawad et al., 2025). This emerging dosage form consists of micrometer-scale projections (<1000 μm) of various geometries that temporarily disrupt the stratum corneum to facilitate drug release into the deeper skin layers while avoiding activation of nociceptors (Alimardani et al., 2021; Dul et al., 2023). They can be subcategorized based on their principal action and manufactured using a range of materials. Dissolving MAPs are typically made from water-soluble polymers such as polyvinyl alcohol, polyvinyl pyrrolidone, cellulose derivatives, chitosan, or sodium hyaluronate. Their drug load capacity is influenced by factors such as needle geometry (shape, height, inter-needle spacing, and area) and composition (Ando et al., 2024; Johnson et al., 2016). Numerous studies suggest that MAPs can enhance nanoparticle permeation into the skin following topical application (Alimardani et al., 2021; Coulman et al., 2009).

However, the manufacturing process for an integrated system that combines dissolving MAPs with nanoformulations, is complex. Systematic methodologies based on risk analysis, such as the Quality by Design (QbD) approach (International Council for Harmonisation, 2009; Simões et al., 2024), are therefore required to identify fundamental challenges and encourage development of quality products. This study aims to formulate a volatile API, β-caryophyllene, in a

nanoemulsion formulation and integrate this within a dissolving MAP to facilitate local delivery following topical application.

2. MATERIALS AND METHODS

2.1 Chemicals and reagents

β-caryophyllene (91.0%), Span® 80, Tween® 20, polyvinyl pyrrolidone (PVP, 40 kDa and 360 kDa), polyvinyl alcohol (PVA, 9 – 10 kDa, 80% hydrolyzed) were purchased from Sigma (St. Louis, MO, USA). Polydimethylsiloxane kit (PDMS, Sylgard™ 184 silicone elastomer kit) was purchased from Dow Corning Corporation (Midland, MI, USA). All other chemicals or reagents were of analytical grade or HPLC grade. Ultrapure water was obtained from Milli-Q apparatus (Millipore).

2.2 Chromatographic conditions

High-performance liquid chromatography with ultraviolet detection (HPLC-UV) (LC-20A; Shimadzu, Nakagyo-ku, Kyoto, Japan) was used to determine the β-caryophyllene content in the arrays and to quantify it in samples from the skin permeation study. The system included an LC-20AT pump, UV-VIS SPD-20A detector, DGU-20A5 degasser, SIL-20A sampler, CBM-20A controller, and a Shim-pack CLC-ODS column (C18, 250 × 4.6 mm, 5 µm; Shimadzu). The chromatographic conditions were validated according to guidelines for analytical and bioanalytical methods (European Medicines Agency, 2022, 2019). The mobile phase consisted of methanol and ultra-purified water (85:15), acidified with 0.1% v/v trifluoracetic acid. The flow rate was maintained in isocratic mode at 1.00 mL/min, with an injection volume of 30 µL. The column oven temperature was set to 40 °C, and detection was performed at 210 nm.

2.3 Preparation and characterization of β-caryophyllene nanoemulsion

The nanoemulsion was prepared using high pressure homogenization (Weimer et al., 2023). The oily phase consisted of β-caryophyllene (20.0% w/w) and Span® 80 (4.0% w/w), while the aqueous phase comprised Tween® 20 (4.0% w/w) and ultra-purified water (q.s. to 100.0% w/w). The oily and aqueous phases were weighed separately, and the aqueous phase was gradually added to the oil phase under continuous stirring. To reduce the droplet size, the mixture was stirred using an Ultra-Turrax disperser (IKA®-Werke GmbH & Co. KG, Staufen, Germany) at 9500 rpm for 1 minute, followed by high-pressure homogenization (EmulsiFlex-C3; Avestin, Ottawa, ON, Canada) for six cycles at 750 bar, without heating.

The droplet size (nm) and polydispersity index (PDI) were measured using dynamic light scattering (Zetasizer Nano ZS90; Malvern Panalytical, Malvern, Worcestershire, UK). Samples were diluted in ultrapure water at a ratio of 1:1000 prior to measurement. Zeta potential (mV) was determined by electrophoretic light scattering using the same equipment, with samples diluted in a 1 mM NaCl aqueous solution (1:1000). The β-caryophyllene content was assessed using HPLC-UV, and the encapsulation efficiency (EE) was determined by ultracentrifugation at 10,000 rpm for 50 min. Aliquots of 500 µL of the nanoemulsion were placed in the upper chamber of centrifuge tubes equipped with an ultracentrifugation membrane (Ultrafree-MC, 10,000 MW; Merck Millipore,

USA) (Kreutz et al., 2021). The equation applied for the calculation of EE is provided below (Eq. 01).

Eq. (01)

$$EE\ (\%) = [(W_{initial} - W_{free}) / W_{initial}] \times 100$$

Where: EE – encapsulation efficiency; Winitial - Total weight of beta-caryophyllene added; Wfree - Weight of caryophyllene quantified in the filtered fraction (free fraction).

2.4 Fabrication of β-caryophyllene-loaded MAP

Pyramidal arrays (10 × 10 microneedles) were created using a masked stereolithography technique (Saturn 2 – 8K; Elegoo, Shenzhen, China). Negative molds were produced from these master molds using polydimethylsiloxane (PDMS) and were subsequently utilized in a two-step cast micromolding process (Mir et al., 2020). Initially, stock dispersions of polyvinylpyrrolidone (PVP) (40 kDa) and polyvinyl alcohol (PVA) (9–10 kDa) were prepared in ultra-purified water at various concentrations (ranging from 10.0% to 50.0% w/w), as outlined during the screening and optimization phases using design of experiments (DoE). The PVP and PVA dispersions were then mixed in predetermined ratios.

Next, the β-caryophyllene nanoemulsion was incorporated into the PVP-PVA polymer mixture under stirring, with the amount of nanoemulsion calculated based on the β-caryophyllene content relative to the dry polymer mass (ranging from 0.03 to 0.15 of β-caryophyllene).

The resulting mixture was uniformly distributed over the PDMS micromolds and placed in a positive pressure chamber (20–30 psi) for 30 minutes. Excess formulation was removed, and the needles were dried for 1 hour at 22% ± 2% relative humidity (RH). Herein, the drying temperature of the needles was applied according to the specification of the full factorial design (detailed matrix in Table S1).

Following this, the base-forming mixture for the microneedle array patch (consisting of 15.0% w/w PVP 360 kDa and 1.5% w/w glycerin) was added, and the molds were subjected to a vacuum environment for 30 minutes. The final drying process was performed at 25 °C with 35% ± 5% RH. Once dried, the arrays were carefully extracted from the molds and stored in sealed aluminum-polymeric film packages.

2.5 Quality by Design approach for development of dissolving MAPs integrated with β-caryophyllene-loaded nanoemulsion

Given the complexity of this system, which involves multiple manufacturing steps, the development process was guided by a systematic QbD approach, supported by quality risk management principles (International Council for Harmonisation, 2009, 2006). The following steps and tools were implemented during development to ensure the feasibility of future translation from prototype to product:

- Establishment of a quality target product profile (QTPP) and defining critical quality attributes (CQAs).
- Identifying the critical material attributes (CMAs) and critical process parameters (CPPs).
- Conducting a risk assessment.
- Performance of a DoE to evaluate the high-risk CMAs and CPPs that could influence product quality.
- Achievement of an optimized formulation and defining the design space to manage variability without compromising product quality.

2.5.1 Establishment of QTPP, selection of CQAs, and initial risk assessment

The QTPP elements, including attributes, targets, and justifications, were drafted based on the specifications of a finished "product" and the pharmaceutical formulation intermediates, using theoretical and practical knowledge of the process (International Council for Harmonisation, 2006). The CQAs were identified from the QTPP. A risk estimation matrix (REM) based on theoretical analysis was then used to define the interactions between CQAs, CMAs, and CPPs; these interactions were subsequently classified as high, medium, or low risk.

2.5.2 DoE: 2^4 full factorial design and Box–Behnken design (BBD)

After generating the REM, interactions between CMAs and CPPs with high-risk CQAs were analyzed, and the essential factors for the DoE were selected. Initially, a 2^4 full factorial design with four factors at two levels was conducted to investigate their effects on β-caryophyllene content (Y_1) and compression force (Y_2). The factors and levels used were: (X_1) percentage of polymers in the dispersion (% w/w): 20.0% and 40.0% w/w, (X_2) β-caryophyllene ratio relative to the polymer solids content: 0.03 and 0.15, (X_3) PVP to PVA ratio: 1.0 and 2.5, and (X_4) needle drying temperature: 25.0 °C and 40.0 °C. These combinations resulted in 16 formulations, as detailed in Table S1 (Supplementary material). The effects of the factors on the dependent variables were analyzed using Pareto and main effects charts following stepwise analysis ($\alpha = 0.15$).

Significant factors affecting β-caryophyllene content in the 2^4 design were included in the second stage of the DoE, with the goal of optimizing the formulation using BBD (3^3) (Politis et al., 2017). The three factors were: (X_1) percentage of polymers in the dispersion (% w/w), (X_2) β-caryophyllene ratio relative to the solids content of the polymers, and (X_3) PVP to PVA ratio. Each factor was evaluated at three levels: 20.0%, 30.0%, and 40.0% w/w (X_1), 0.03, 0.09, and 0.15 (X_2), and 1.0, 1.75, and 2.5 (X_3). The dependent variable, β-caryophyllene content (Y_1), was measured by HPLC-UV. This randomized design involved 15 combinations, as shown in Table S2. Data were analyzed using linear regression followed by a second-order polynomial model (Eq. 02). Statistical analyses were performed using Minitab® 17.1 software, with least-squares regression and analysis of variance (ANOVA) to determine linear, quadratic, and interaction coefficients at a 5.0% significance level.

Eq. (02)

$$Y = A_0 + \sum_{i=1}^{k} A_i X_i + \sum_{i=1}^{k} A_{ii} X_i^2 + \sum_{i=1}^{k-1} \sum_{j=1+1}^{k} A_{ij} X_i X_j$$

Where: the regression coefficients of constant, linear, quadratic, and interactions terms are represented respectively by A_0, A_i, A_{ii}, and A_{ij}. k is the number of variables, and the independent variables are represented by X_i, X_j, and X_k.

Following data analysis and stepwise ($\alpha = 0.15$) analysis to generate the final equation, formulation optimization was simulated in the same software (Minitab® version 17.1), prioritizing the maximization of β-caryophyllene content. The X_2 factor was fixed at 0.09, with no restrictions on X_1 and X_3. Equal weighting was applied to all independent variables, and the desirability (d) prediction coefficient was evaluated. Finally, the software predicted optimized conditions were experimentally validated and fully characterized. A design space was generated that established a β-caryophyllene content within a range of 90.0% to 105.0%.

2.6 Characterization of optimized dissolving MAPs containing nanoemulsified β-caryophyllene

2.6.1 Determination of MAP β-caryophyllene content

The β-caryophyllene content of MAPs was determined using HPLC-UV under the chromatographic conditions previously described. Standard curves of β-caryophyllene (25.0 to 500.0 µg/mL) were prepared in methanol. MAP samples were initially dissolved in 1 mL of ultra-purified water, followed by the addition of 9 mL of methanol. All samples were filtered through 0.45 µm PVDF syringe filters before HPLC analysis. The β-caryophyllene content was expressed as a relative percentage (± standard deviation).

2.6.2 Mechanical strength

The mechanical strength of the MAP formulations were evaluated under compression using a texture analyzer (TA-XT plus; Stable Micro Systems, Godalming, Surrey, UK) (Permana et al., 2019). The samples were secured to a P/10 probe with double-sided tape, and a perpendicular force was applied at a constant compression speed against a heavy-duty platform. The test parameters were set to compression mode, with a test speed of 2.0 mm/s, pre-test and post-test speeds of 1.0 mm/s, a compression distance of 0.4 mm, and a trigger force of 32.0 N. After the test, the maximum compressive force sustained by the MAPs was recorded in the Exponent software, based on the force (Y) versus time (X) plot.

2.6.3 Dynamic light scattering and morphology analysis

Dynamic light scattering was used to compare the size and polydispersity index (PDI) of the nanodroplets before and after mixing with polymers. TEM (120 keV, JEM-1400, JEOL Inc., USA) was used to examine the morphology of the β-caryophyllene nanoemulsion before and after mixing

with the polymer dispersion, as well as to investigate the presence of nanodroplets following MAP dissolution. For TEM analysis, samples were diluted in water (1:20 v/v), fixed on formvar-coated copper grids (200 mesh), and contrasted with 2.0% w/v uranyl acetate.

The morphology of the MAPs was assessed using four techniques: digital microscopy, transmission electron microscopy (TEM), scanning electron microscopy (SEM), and X-ray microcomputed tomography (XμCT).

Digital microscopy (ISKAM-315; Shenzhen Inskam Company Ltd., Shenzhen, China) was employed for real-time monitoring of the micromolding process to ensure proper filling of the microcavities. It also served as a quality control method for the demolding process, general appearance of the arrays, assessment of *in vitro* skin insertion, and in *vitro* dissolution time.

The dimensions of MAPs were assessed by SEM (EVO MA10; Zeiss, Oberkochen, Germany). Samples were mounted at a 90º angle on stubs with double-sided carbon tape and coated with gold. The microscope was operated at 10.0 kV, and images were captured at magnifications ranging from 50 to 150×.

The porosity of MAPs was assessed using XμCT (SMX-90 CT; Shimadzu). Imaging was performed at 70 kV and 90 mA, with 4800 views and a resolution of 1024 × 1024. The source–object distance was set to 22.0 mm. Images were reconstructed using InspeXio SMX-90CT software (Shimadzu).

2.6.4 In vitro skin insertion

MAP skin insertion capacity was evaluated using a texture analyzer (TA-XT plus; Stable Micro Systems) to apply MAPs at a controlled speed and force in two *in vitro* models: (i) Parafilm® layers and (ii) porcine ear skin (Larrañeta et al., 2014; Permana et al., 2021). The separation of the skin from the porcine ear skin followed the methodology described in a previous study (Lucca et al., 2020).

For both techniques, the MAPs were affixed to a P/10 probe with double-sided tape and pressed perpendicularly against either (i) eight overlapping Parafilm® layers (1.0 cm^2, 1.0-mm thickness) or (ii) porcine ear skin (0.9- to 1.1-mm thickness). The texture analyzer was operated in compression mode with the following parameters: test speed of 2.0 mm/s, pre-test and post-test speeds of 1.0 mm/s, trigger force of 32.0 N, and hold time of 30 seconds.

After testing, the Parafilm® layers were analyzed individually using digital microscopy (ISKAM-315; Shenzhen Inskam Company Ltd.) to examine penetrations that were consistent with the pattern of the 10 × 10 microneedle array. Porcine skin was also analyzed via digital microscopy and post-stained with 0.4% trypan blue solution to visually determine insertion performance i.e. the percentage of needles that punctured the skin.

2.6.5 In vitro and ex vivo MAP dissolution

The kinetics of MAP dissolution was evaluated using two different environments (i) *in vitro* (in buffer solution) and (ii) *ex vivo* (using porcine ear skin). In the first *in vitro* method, 2 mL of phosphate-buffered saline (PBS) (pH 7.4) was added to a beaker, and the array was fixed in a Petri dish so that only the needles contacted the buffer solution, which was agitated at 20 rpm. The time

for complete microneedle dissolution was determined by digital microscopy (ISKAM-315; Shenzhen Inskam Company Ltd.) following their removal from the dissolution medium.

In the second (*ex vivo*) method, MAPs were applied to porcine skin (isolated from the ear), supported by cork, with a standardized force of 32.0 N for 5 min using a digital force gauge (FH 100, Sauter GmbH, Germany). The hydration of the skin was maintained by PBS (pH 7.4). Optical coherence tomography (OCT) (Michelson Diagnostics Ltd, UK) was used to acquire scans in a real-time immediately after MN insertion and at 1, 2, 4, 6, and 12 hours post-application. The OCT system used in this study was a multi-beam swept-source frequency domain VivoSight™ with an axial resolution of <10 µm and lateral resolution of <7.5 µm. Each scan consisted of 500 frames with a scan width of 6 mm.

The scans were analyzed using the imaging software ImageJ® (National Institute of Health, USA). Transverse sections were post-processed using ImageJ® to determine the depth of microneedle insertion, the distance between the skin surface and the base of the MAP, and the extent of needle insertion into the skin.

2.6.6 In vitro skin release of β-caryophyllene

For the evaluation of delivered dose of β-caryophyllene after 24 h of MAPs skin insertion , MAPs were applied perpendicularly to the central region of dermatomed (0.9 to 1.1 mm in thickness) porcine skin using a texture analyzer (32.0 N for 30 seconds), after which the skin was mounted in static Franz-type diffusion cells (OCDE 428, 2004). The receptor fluid composition was validated beforehand to ensure sink conditions (data not shown). Each Franz cell contained 10 mL of receptor phase liquid, consisting of 79.6% v/v PBS (pH 7.4), 20.0% v/v HPLC methanol, and 0.4% v/v Tween® 80, maintained at 37 °C. MAP treated porcine skin (n = 6) was compared to topically treated skin (n = 6), using a simple dose matched liquid β-caryophyllene-loaded nanoemulsion (6 µL). The remaining base of the arrays (n = 6) was removed after 24 hours using tweezers and sterile gauze moistened with PBS (pH 7.4), without damaging the stratum corneum.

At the end of the test (24h), 1 mL of receptor fluid was collected, filtered through 0.45 µm PVDF membranes, and analyzed for β-caryophyllene concentration using HPLC-UV. In addition, all skin samples were removed, cleaned with purified water and dried with cotton wool to remove any excess caryophyllene not retained in the skin. Then, the whole skins were dissected into small pieces and transferred to amber vials, to which 1 mL of HPLC methanol was added before a 30 min sonication to extract the β-caryophyllene. The resulting liquid was filtered and analyzed via HPLC-UV. The results were expressed as the average mass of β-caryophyllene in the fluid and skin sample, ± standard deviation.

2.6.7 Water activity

The water activity (aw) of optimized MAPs was measured using the dew point technique in a water activity analyzer (PRE; Aqualab, Pullman, WA, USA). For this test, arrays up to 20 days after manufacture were used.

2.7 Preliminary stability study

Optimized MAPs were stored in aluminum sachets sealed with a polymeric film. Samples were kept at room temperature (25 °C ± 5 °C, 40% ± 10% RH) and β-caryophyllene content, mechanical strength and *in vitro* skin insertion capacity (using the Parafilm® technique) was analysed at the following timepoints 1, 30, 45, and 60 days (n = 3/timepoint). Additionally, the mass of the MAPs was recorded during the storage period.

2.8 Statistical analyses

Statistical analyses for the DoE were conducted using Minitab® version 17.1 (Minitab Inc., State College, PA, USA). Regression models in the full factorial design and BBD were adjusted stepwise to include only the significant terms ($p < 0.05$) in the final equation. The stepwise adjustment process was monitored by evaluating the coefficient of determination (R^2) and adjusted coefficient of determination (R^2-adj) before and after excluding terms (data not shown). For the BBD, the lack-of-fit test was performed using ANOVA ($p \leq 0.05$).

For other assays, statistical analyses were performed using GraphPad Prism software (version 6.0), applying an unpaired Student's t-test and one-way ANOVA with post hoc Tukey tests ($p < 0.05$), after confirming a normal data distribution.

3. RESULTS AND DISCUSSION

3.1 Preparation and characterization of a β-caryophyllene nanoemulsion

The high molecular weight and lipophilic nature of β-caryophyllene (National Center for Biotechnology Information, 2019) is most suited to a nanoemulsion formulation, where in a dispersed system the droplet phase exists as nanometer-scale droplets that are stabilized by surfactants (Rai et al., 2018). Unlike other nanosystems, that usually present medium-chain triglycerides (MCT) in the oil core, β-caryophyllene can serve as the oily core in oil/water nanoemulsions, allowing for a higher drug load.

In this study a β-caryophyllene nanoemulsion was successfully produced by high-pressure homogenization and possessed a droplet size of 152 ± 1 nm, a PDI of 0.12 ± 0.02, and a zeta potential of −35.2 ± 1.2 mV (n = 3). These values indicate that the emulsion formulation is homogeneous (droplet size < 500 nm, PDI < 0.30) with a low tendency for droplet aggregation (zeta potential > |30| mV) (Danaei et al., 2018; Singh et al., 2017). Quantitative analysis indicated a β-caryophyllene content of 98.5% ± 1.2%, relative to the initial amount added, with an EE of 96.5% ± 1.3%.

3.2 Fabrication of nanoemulsified β-caryophyllene-loaded MAP

Previous studies have exemplified incorporation of a range of nano-formulations within dissolving MAPs, including polymeric, phospholipid, and inorganic systems (Mir et al., 2020; Permana et al., 2021; Srivastava and Thakkar, 2021; Volpe-Zanutto et al., 2021). In this study, the masked stereolithography technique was used to produce the master mold, followed by the creation of female PDMS micromolds.

PVA and PVP combinations were selected for dissolving MAP manufacture because of their biodegradability and biocompatibility, as well as the wide range of molecular weights and hydrolysis grades (Li et al., 2024; Permana et al., 2020; Sheskey et al., 2020) that are available, which enables tailoring of the formulation. Iterative development and optimization resulted in the selection of PVA 9–10 kDa (80% hydrolysis) and PVP 40 kDa for needle manufacture, while PVP 360 kDa was selected for the baseplate. Polymeric dispersions of PVP and PVA ranging from 10.0% to 50.0% w/w and PVP:PVA ratios from 1.0 to 2.5 were used to manufacture microneedles, and their integrity was evaluated using digital microscopy. A 10.0% w/w polymer dispersion resulted in fragile needles and incomplete mold filling, while dispersions with a concentration of more than 40%v/v had a high viscosity (Fig. S1), which hindered proper filling of the microcavities. Rheological studies indicated that increasing the PVP:PVA ratio from 1.0 to 2.5 could reduce viscosity (Fig. S1). Mathematical modeling and rheogram analysis (shear rate vs. shear stress) confirmed Newtonian fluid behavior for all dispersions (Bingham, Ostwald, and Herschel–Bulkley; r = 1.00), and this was unaffected by the addition of β-caryophyllene nanoemulsion.

Homogeneity tests were conducted on polymer dispersions after mixing with the nanoemulsified β-caryophyllene formulation. Low and high factor values were evaluated: (i) polymer dispersion concentration (20.0% and 40.0% w/w), (ii) PVP:PVA ratio (1.0 and 2.5), and (iii) nanoemulsified β-caryophyllene ratio in relation to the solids content of the polymers (0.03 and 0.15). After homogenization, the macroscopic appearance of the mixtures was recorded over a period of 6 hours (Figs. S2 and S3). A higher PVP:PVA ratio (2.5) resulted in lower viscosity and increased phase separation (Fig. S3(D)) compared to a PVP:PVA ratio of 1.0 (Fig. S2(D)). Additionally, a 40.0% w/w polymer mixture maintained uniformity longer than 20.0% w/w dispersions (Figs. S2 and S3(D–F)).

Phase separation occurred after 2 hours, with β-caryophyllene accumulating in the upper portion due to its density, promoting content loss through evaporation. Based on these findings, the micromolding process should limit the time between the first and second casting steps to 1 hour. Furthermore, the impact of RH on drying time was evaluated (data not shown). Optimal conditions were determined to be 22% ± 2% RH for needle drying and 35% ± 5% RH for base drying.

3.3 Quality by Design considerations

3.3.1 Quality Target Product Profile and Risk Estimation Matrix

In recent decades, the pharmaceutical industry has implemented a systematic approach to product and process development based on risk analysis, known as QbD. QbD tools and elements are employed from the initial development stage to ensure product quality; define acceptable variations within the production process, including material and process attributes; and predict the product's life cycle while promoting cost minimization (International Council for Harmonisation, 2009, 2006; Simões et al., 2024).

A QTPP was established for the QbD-driven development of dissolving MAPs integrated with β-caryophyllene nanoemulsion. According to the ICH Q8(R2) guideline, the QTPP forms the foundation of pharmaceutical product development, guiding the choice of production processes and formulation criteria and determining CQAs for risk monitoring tools (International Council for Harmonisation, 2009). Table 1 lists the elements, targets, and justifications, identifying which elements and targets are considered CQAs.

391

392 Table 1 - Identification of quality target product profile (QTPP) and critical quality attributes (CQAs) for the dissolving
393 microneedle integrated with β-caryophyllene nanoemulsion and for the pharmaceutical formulation intermediates

Element	CQA	Target	Justification
Administration route	No	Transdermal	Absorption of β-caryophyllene at higher concentrations than oral and topical routes and possibility of controlling release. Application close to the inflammatory site.
Dosage form	No	Dissolving microneedle integrated with β-caryophyllene nanoemulsion	
Clinical indication*	No	Reduction of chronic pain symptoms associated with inflammatory conditions	β-caryophyllene is a multitarget compound which acts on type 2 endocannabinoid receptors (CB2) and modulates inflammatory mediators (Klauke et al., 2014; Sharma et al., 2016). Thus, the release of this compound close to the inflammatory site may confer benefits in the management of chronic pain associated with inflammatory conditions such as osteoarthritis. *
Drug delivery matrix	No	Hydrophilic	Delivering of the nanoemulsified bioactive compound from a hydrophilic, biocompatible, and biodegradable polymeric matrix. After skin insertion, the matrix underwent a process of hydration and dissolution, gradually releasing the nanoemulsified β-caryophyllene.
Quality attributes			
PFI Physical attributes (color, odor, and appearance)	No	Slightly viscous, homogeneous, opaque, white to yellowish liquid with a slight odor of β-caryophyllene odor. No phase separation should be observed after 1 hour at rest.	The addition of the nanoemulsion to the polymeric dispersion changes the color to white and slightly reduces the viscosity. The separation

				of the oily phase (API) and the aqueous phase (polymers) can be favored when polymeric dispersions with low viscosity values and high levels of nanoemulsified β-caryophyllene are applied. Keeping the uniformity for 1 hour at rest is relevant to the micromolding process. Although not classified as a CQA, any changes in physical characteristics should be investigated.
	Nanometric characteristics	Yes	Droplet size <400 nm Polydispersity index <0.50	Nanometric characteristics to promote the stability of β-caryophyllene and its uniformity in the polymer matrix.
	Viscosity	Yes	From 200 c*P* to 3000 c*P***	The viscosity is directly related to the concentration of the polymers and the combination ratio between PVA and PVP. Furthermore, this parameter must be controlled as it has an impact on the mold filling stage.
FPF	Physical attributes (color and appearance)	No	Flat base (1 cm^2), translucent, and slightly yellowish with projections in the shape of pyramidal needles, opaque white in color.	By visual analysis, the base made up of PVP and adjuvant should appear homogeneous and translucent. The needles, due to the presence of nanoemulsified β-caryophyllene, should be white and opaque. Although not classified as a CQA, any changes in physical characteristics should be investigated.
	Drug load#	Yes	Maximize	Increasing the concentration of β-caryophyllene absorbed and potentiating the therapeutic effect.
	Stability of the β-caryophyllene	Yes	Maximize (>90% β-caryophyllene content)	Ensure the stability of β-caryophyllene and avoid possible losses through

content after micromolding			volatilization during the micromolding process.
Geometric microstructure	Yes	Pyramidal needles; height: 500–1000 µm; inter-needle base spacing: 200–800 µm; tip diameter: 20–70 µm; density: ≥ 100 needles/cm².	The geometry of the microneedles should allow insertion into the skin up to the epidermis while enabling drug loading compatible with therapeutic efficacy. Skin insertion is influenced not only by the material composition but also by geometric parameters, including base and tip inter-needle spacing, needle height, tip diameter, base width, needle shape, and needle density.
Microneedle integrity	Yes	Completely filled matrix (10 × 10 needles/array) with no fractures in the microstructure	The integrity of the matrix is necessary for complete skin insertion and maintenance of the optimized drug load.
Compression force	Yes	Sufficient to promote skin insertion (>50 N/array) (Larrañeta et al., 2014)	Ensure optimum compression force for skin insertion without needle breakage.
*S*kin insertion profile	Yes	Complete insertion of the MAP by applying manual force	Uniform insertion of the matrix (e.g. 10 × 10), representing the rupture of the stratum corneum (15 µm) and penetration of the epidermis.
Dissolution time profile	Yes	Complete dissolution of the needles during the prescribed period of use	To promote the release of nanoemulsified β-caryophyllene.
Water activity	No	Minimize without compromising the ideal mechanical characteristics for full insertion of the matrix into the skin	The reduced water activity in allows the control of a low bioburden and consequently reduces the risk of infection during application. (Dul et al., 2023)
Transdermal absorption	Yes	Promote prolonged release system	Prolonged effect to better adapt the dosage to the chronicity of the clinical indication (once-daily)

Stability	Yes	12 months	Quality requirement to be performed by the optimized formulation in order to ensure safety and efficacy.
Packaging closure system	No	Aluminum sachets with sealed polymeric film	An inert packaging that protects from humidity is necessary to guarantee its integrity, mechanical characteristics for skin insertion, and stability of the β-caryophyllene content during shelf life. The packaging must also be easy for the patient to handle.

API: Active Pharmaceutical Ingredient; EE: entrapment efficiency; FPF: final pharmaceutical formulation, dissolving microneedle integrated with β-caryophyllene nanoemulsion; PFI pharmaceutical formulation intermediate - polymer blend containing β-caryophyllene nanoemulsion; PVA: polyvinyl alcohol; PVP: polyvinyl pyrrolidone.

*The prototype of the dissolving microneedle integrated with the β-caryophyllene nanoemulsion was developed with the aim of being applied in clinical cases of chronic pain associated with inflammatory conditions. Firstly, its development process was based on the international Quality by Design guidelines and well documented in this article. Its clinical efficacy will be reported in specific documents for these trials. **Viscosity values obtained at 20 rpm, spindle number 18, Brookfield Rotational Viscometer, model DV-II+.

Usually, the QTPP is developed for the final pharmaceutical product. However, because of the specificities of the integrated system and the production of three intermediate products that directly affect quality, these intermediates were also detailed in the QTPP (Table 1). The intermediate pharmaceutical formulation (PFI) represents the mixture of polymeric dispersion with the nanoemulsion, respectively. The quality criteria of the final product are directly influenced by PFI because this intermediate is transferred to the micromolds and subjected to the drying process. After developing the QTPP, it became evident that the DoE should include variations in PFI's composition and process criteria. The optimized formulation should then be characterized according to the elements of the final formulation (FPF) and meet the pre-established targets.

CQAs are defined as properties or characteristics of a chemical, physical, biological, or microbiological nature that must remain within specific limits to ensure product quality, and consequently, safety and efficacy (International Council for Harmonisation, 2009). CQAs can apply to the materials (active pharmaceutical ingredient [API], excipients, and packaging) and the process. Considering the development of MAPs towards commercial products, and the need for regulatory guidance around MAP development and testing, the Microneedle Array Patch Regulatory Working Group has established a list of CQAs for these systems (MAP RWG, 2024). The biological attributes were categorized into biocompatibility and delivered dose, while microbiological attributes were divided into microbiological specification, water activity, and particulates. Chemical attributes include chemical stability, assay, content uniformity, drug purity, dissolution, and water content. Physical attributes encompass the container closure system, mechanical strength, puncture performance, and needle morphology (Dul et al., 2025).

Considering that CMAs and CPPs directly impact CQAs (International Council for Harmonisation, 2006), a risk assessment was conducted using a REM tool. Tables S3 and S4 present the REM for CMAs versus CQAs and CPP versus CQAs, respectively.

As shown in Table S3, 10 high-risk interactions were identified between the CQAs and CMAs related to the API (β-caryophyllene) and polymers. Of these, factors that could be modulated and measured through DoE were selected. These factors were the concentration of the API, the concentration of the polymers in dispersions, and the combination ratio of the polymers. Other high-risk interactions were monitored. In Table S4, the CPP chosen for evaluation by full factorial design was the needle drying process, specifically the drying temperature, because of the volatility of β-caryophyllene. Also, to study the interactions between CMAs, CPPs, and their influence on CQAs, the QbD methodology involved applying DoE alongside preliminary risk analysis (Simões et al., 2024).

3.3.2 Design of Experiments

The screening DoE in this study was a two-level full factorial design, which allowed for the measurement of main effects, interaction effects, and quadratic effects by testing combinations of all factors (X_1, X_2, X_3) at both levels (−1, +1) (Simões et al., 2024). Stepwise regression was applied to adjust the regression models, and R^2 and R^2-adj values were compared before and after the adjustment. For both outputs—β-caryophyllene content (Y_1) and compression force (Y_2)—the fit of the coefficients of determination improved. The R^2 and R^2-adj for β-caryophyllene content were 0.9247 and 0.8587, respectively. For compression force, R^2 was 0.9529 and R^2-adj was 0.7646. These values were considered acceptable for the purpose of verifying the factor effects and determining which factors to include in the optimization DoE.

Figure 1 presents Pareto charts and main effects charts for the full factorial design. As shown in Figure 1A, polymer solids (X_1), the interaction with the β-caryophyllene ratio (X_1X_2), and their interaction with the PVP:PVA ratio ($X_1X_2X_3$) influenced the β-caryophyllene content output. The needle drying temperature had no significant effect. This supports the findings from the homogeneity studies (Section 3.2), in which increasing the polymer concentration from 20.0% to 40.0% w/w increased the β-caryophyllene content, while increasing the PVP:PVA ratio from 1.0 to 2.5 slightly reduced the content.

The compression force output (Fig. 1B, D) was influenced by all factors, but nominal compression force values did not affect puncture efficiency because all experiments resulted in forces above 132 N. A study involving volunteers indicated that manual force applied during application ranged from 10 to 50 N (Larrañeta et al., 2014); thus, the dissolving MAP was designed to withstand up to 50 N of compression force. Given these results, DoE optimization focused on the β-caryophyllene content. The BBD was applied, allowing for the evaluation of main, interaction, and quadratic effects. The use of BBD supports a more sustainable approach in scientific research by reducing the number of experiments, thus minimizing resource consumption and waste (Politis et al., 2017).

Figure 2 shows the results of BBD. The model showed no lack of fit ($p = 0.140$), and the coefficients of determination after stepwise regression were $R^2 = 0.8952$ and R^2-adj = 0.8370. The regression equation for the model is provided in Eq. (02).

Eq. (02)

$$\beta\text{-caryophyllene content (\%)} = -133.7 + 4.201\ X_1 + 643\ X_2 + 73.6\ X_3 - 5455\ X_2^2 - 23.7\ X_3^2$$

Where: (X_1) percentage of polymers in the dispersion (% w/w), (X_2) β-caryophyllene ratio in relation to the solids content of the polymers, and (X_3) PVP:PVA ratio.

The contour plots (Fig. 2A–C) indicate that β-caryophyllene contents above 90.0% can be achieved with the following conditions: (X_1) polymer concentration between 35.0% and 40.0% w/w, (X_2) car:polymer ratio between 0.03 and 0.10, and (X_3) PVP:PVA ratio between 1.2 and 2.1. These area conditions can be verified in the navy-blue regions on the contour plots. It can also be verified by the white area marked in Fig. 2-D.

To verify the optimization conditions, three scenarios were generated using Minitab® 17.1 software, with the highest desirability value (d = 1.000) chosen. The optimized conditions were (X_1) polymer solids at 40.0% w/w, (X_2) β-caryophyllene ratio at 0.09, and (X_3) PVP:PVA ratio at 1.54. This composition was used for microneedle production and further characterization of the array. It is important to note that the baseplate composition remained constant throughout testing (15.0% w/w PVP 360 kDa + 1.5% w/w glycerin), and the microneedles were dried at 40 °C for 1 hour (22% ± 2% RH) before adding the base.

3.4 Characterization of optimized dissolving MAP integrated with nanoemulsified β-caryophyllene

3.4.1 Determination of MAP β-caryophyllene content and mechanical strength

The formulation optimized through DoE met the quality profile outlined in the QTPP (Table 1). The average mass of β-caryophyllene loaded into the array was 1235 µg, with a content of 95.96% ± 1.45%. This result demonstrates that optimizing the formulation by combining the nanoemulsified system with MAP retarded the loss of β-caryophyllene through volatilization. Furthermore, despite the β-caryophyllene being liquid at storage temperature, which could cause the MAP to become fragile, the optimization resulted in a mechanical strength (129.9 ± 9.2 N) compatible with the theoretical value estimated for promoting skin penetration.

3.4.2 Dynamic light scattering and morphology analysis

For the nanometric characteristics of β-caryophyllene nanoemulsion) and PFI (β-caryophyllene nanoemulsion in polymer dispersion), the average droplet size (PDI) increased from 152 ± 1 nm (0.12 ± 0.02) to 398 ± 1 nm (0.45 ± 0.04), as measured by dynamic light scattering. In addition to dynamic light scattering, the nanoemulsion, PFI, and the final formulation after dissolution were analyzed by TEM (Fig. S4). These data showed that nanodroplets of similar size were observed in β-caryophyllene nanoemulsion (Fig. S4A) and after dissolving the array (Fig. S4C, D), but they were not clearly visible in PFI (Fig. S4B), as the circular structures seem to be artefacts often found in TEM, also observed in Fig. S4A along with nanodroplets. These findings further suggest that analyzing dissolving MAPs integrated with nanosystems is complex and requires multiple techniques, and that future improvements in existing methods are needed.

In a scoping review conducted by our research group on the characterization of dissolvable MAP associated with nanostructured systems, we observed that fewer than 30% of the studies analyzed evaluated the size and morphology of the nanostructures after their incorporation into the MAP (Weimer et al., 2021). The primary reason reported for this limitation was the interference of polymeric matrices with conventional particle size characterization techniques. Furthermore, the incorporation of nanoemulsions into dissolvable microneedles remains scarcely explored in the literature, with most studies focusing predominantly on the feasibility of formulation and device development (Ali et al., 2024; Nasiri et al., 2022). Therefore, further investigations addressing the interactions and physicochemical phenomena between nanodroplets and the polymeric matrix are warranted.

MAPs (10 × 10 needles) were formed by micromolding, resulting in pyramidal needles (Fig. 3A, B). SEM analysis (Fig. 5) confirmed the geometry and dimensions of the microneedles, with no significant differences between MAPs made from polymers alone (blank) (Fig. 5A) and those containing β-caryophyllene nanoemulsion (Fig. 5B). The optimized formulation resulted in microneedles measuring 916 µm in height, 542 µm in base width, and 61 µm in tip diameter; with 1000 µm and 425 µm interneedle spacing at the tips and bases, respectively; and with a 106º angle between the baseplate and the needle. The pyramidal morphology was confirmed by X-ray microcomputed tomography (XµCT; Fig. 5C), with slight porosity also observed (Fig. 5D).

3.4.3 In vitro skin insertion and MAP dissolution

Several studies have shown that MAP skin insertion efficiency is related to microneedle array design, including factors such as height, shape, aspect ratio, patch area, and interneedle spacing (Johnson et al., 2016; Makvandi et al., 2021; Olatunji et al., 2013). Despite the pyramidal geometry of the optimized MAPs, which could present points of fragility, a compression force exceeding 50.0 N (QTPP) (Table 1) indicated sufficient insertion capacity. This was confirmed using the Parafilm® and porcine ear skin as substrates (Fig. 3C, D).

As shown in Figure 3C, the optimized array achieved 100% penetration of the first Parafilm® layer and approximately 97% of the second layer. Insertion efficiency decreased with the remaining layers, with 11% perforation in the fifth layer. The total insertion depth reached 625 µm, sufficient to penetrate the stratum corneum (10–20 µm) and epidermis/dermis (<800 µm) (Benson and Watkinson, 2012). Penetrations in porcine ear skin after application and removal are shown in Figure 3D. In this substrate, the MAPs showed penetration rates between 92 and 100%. This result was corroborated by the OCT scans, which indicated a penetration depth of approximately 610 µm (67% the total height; Fig. 4A).

Dissolution time analysis revealed rapid dissolution of the microneedles in PBS (pH 7.4) within 16 ± 2 seconds, with complete dissolution in the skin after 12 hours of contact (portion penetrated into the skin, Fig. 4). The OCT technique was used to check the depth of needle insertion and to monitor the dissolution profile in skin. As shown in Figure 4 (A, B), there was a significant reduction in the area in contact with the skin only at 12 hours. Further studies could be carried out in association with imaging techniques such as XµCT to better understand the dissolution mechanism. In addition, the OCT technique indicated that approximately 33% of the needle did not come into contact with the skin. Although it is estimated that two-thirds (605 ± 26 µm) of the total height of the needle will come into contact with the skin, adjustments to needle geometry and interspacing, for example, could be explored in the future to increase the depth of skin penetration.

The dissolution time in the skin correlates with the polymer concentration used in manufacturing and the needle size. Future studies could evaluate the therapeutic effects of β-

caryophyllene in chronic inflammatory conditions like osteoarthritis. A recent *in vivo* study demonstrated 72-hour tissue retention of diclofenac delivered via nanosuspension in PVA/PVP MAPs as a strategy for prolonged pain relief (Li et al., 2024).

3.4.4 In vitro skin release of β-caryophyllene

Transdermal delivery of β-caryophyllene into the receptor compartment was observed only with MAP administration (Table 2). Previous studies using topical nanoemulsified β-caryophyllene, resulted in API deposition within the skin (Peterle et al., 2020; Weimer et al., 2022). Whilst topical application of the nanoemulsion can facilitate skin penetration into the epidermis and dermis, it does not result in complete release through the tissue. In this study, transdermal delivery of β-caryophyllene was achieved through integrating the nanoemulsion with dissolving MAPs.

Table 2 – *In vitro* skin released amount of β-caryophyllene after 24 h of administration of optimized formulations of microneedle and nanoemulsion.

Sample	Optimized microneedle	Nanoemulsion
Whole skin	647 ± 52 µg*	864 ± 133 µg
Receptor fluid	320 ± 41 µg*	< LOQ

LOQ: Limit of quantification. Results expressed as mean mass of β-caryophyllene ± standard deviation. Statistical analysis: Student's t-test *p < 0.05, comparison between optimized microneedle and nanoemulsion.

Regarding oral administration, a human study evaluated pharmacokinetic parameters after taking 100 mg of free β-caryophyllene and found a maximum concentration of 58.2 ng/mL (95% CI: 45.13–71.3 ng/mL). When delivered using a self-emulsifying drug delivery system, the same dose achieved a maximum concentration of 204.6 ng/mL (95% CI: 167.2–242.1 ng/mL) (Mödinger et al., 2022). A direct comparison with the MAP proposed in this work is not possible. However, the concentration measured in the receptor fluid indicates an innovative alternative to oral administration. Additionally, considering the intended clinical application in the QTPP (Table 1), the MAP could be applied near the inflammation site, and dose adjustments could be made, for example, by increasing the patch size. These ideas will be tested in future studies.

3.4.5 Water activity

The last quality parameter evaluated was water activity (aw). Analysis of the entire microneedle array yielded an aw value of 0.34 ± 0.03. As yeast and pathogenic bacterial growth is favored at aw values above 0.60 and 0.75, respectively, this indicates a low potential for microbial growth in the dissolving MAP. Determining the water content and water activity of dissolving MAPs will support the regulatory dossier, enabling the specification of water limits that will

prevent microbial growth or reduce the risk of clinical infection. Ongoing and future clinical studies should consider such measurements to ameliorate potential infection risks associated with the use of MAPs (Dul et al., 2023; MAP RWG, 2024).

3.5 Preliminary stability study

A preliminary stability study was conducted to confirm the maintenance of β-caryophyllene content, compressive force, and *in vitro* skin insertion capacity for the optimized array stored in aluminum packaging with polymeric film. The results are shown in Figure 6. The β-caryophyllene content remained stable for 45 days (Fig. 6A). The stability of the β-caryophyllene content parameter can still be improved, considering the 12-month target established in the QTPP. Future studies may explore additional temperature and humidity ranges beyond those already evaluated (25 °C ± 5 °C, 40% ± 10% RH), as well as potential adjustments to the packaging system.

In a study evaluating dissolvable MAP for the delivery of amoxicillin sodium, it was observed that the drug content was influenced by the type of packaging material employed (McAlister et al., 2021). For formulations containing volatile compounds, additional precautionary measures may therefore be required. Future studies aimed at redefining packaging strategies for MAP containing volatile compounds will include the investigation of a dual-packaging system. For instance, the MAP may be housed in a plastic support and subsequently enclosed within an aluminum package. Additional variables, such as the sealing method, as well as the need of storage in refrigerator before use (e.g. long-term storage of unopened insulin) may also be systematically evaluated.

It is important to emphasize that the 45-day result does not invalidate the proof of concept regarding the delivery of a lipophilic and volatile API in a dissolving MAP. Moreover, we hypothesize that delivering a lipophilic API in nanostructured systems aids in uniform matrix distribution, stability, and action potentiation - all important factors during development.

No statistical differences were observed across time points for compression force (Fig. 6B) or insertion efficiency (Fig. 6C). The array's weight showed a consistent variation of approximately 1.0%–0.5% (Fig. 6D). These results suggest that despite β-caryophyllene's vapor pressure promoting evaporation, β-caryophyllene content was maintained above 90.0% for 45 days. The packaging also ensured the stability of other variables, protecting the array from humidity.

CONCLUSIONS

This study's novelty lies in the successful transdermal delivery of β-caryophyllene using a nanoemulsion formulation integrated in a dissolvable MAP. The results demonstrate that the physicochemical challenges that typically hinder delivery of lipophilic volatile compounds from water-soluble MAPs can be addressed using nanotechnology and a QbD approach. The optimized formulation met the fundamental pre-determined quality criteria i.e. a MAP β-caryophyllene content of over 90% relative to the initial amount added, a reasonable skin insertion force and stability on storage. These results could serve as a foundation for the intra- or transdermal delivery of other terpenic compounds using dissolvable MAPs. Finally, this system holds potential for future studies investigating its use in treating chronic inflammatory pain.

Supporting information

The following files are available as supplemental material (PDF). Experimental section of rheological behavior. Supplementary tables of randomized experimental matrix for 2^4 Full Factorial Design, Box–Behnken Design and risk estimation matrix. Supplementary figures - rheograms of polymeric dispersions, macroscopic appearance of polymeric dispersion containing nanoemulsion, residual plots of 2^4 Full Factorial Design and Box–Behnken Design, and transmission electron microscopy.

DECLARATIONS

Consent for publication: The authors declare that they know of no competing financial interests or personal relationships that may have influenced the work reported in this paper.

Acknowledgements: This work was financially supported by Conselho Nacional de Desenvolvimento Científico e Tecnológico – CNPq, Fundação de Amparo à Pesquisa do Estado do Rio Grande do Sul – FAPERGS, and Coordenação de Aperfeiçoamento de Pessoal de Nível Superior. The authors would like to thank Professor Dr. Eduardo César Tondo and Giulia Giugliani Reta for their support in the water activity analysis. In this study, Dr Maria Dul (co-author), Professor James Birchall and Dr Sion Coulman (Cardiff University) supported the OCT imaging of microneedles in excised porcine skin.

Competing interests: The authors declare no conflict of interest.

Authors' contributions: P. Weimer: Conceptualization, validation, formal analysis, investigation, resources, writing original draft, and project administration. **I. M. Bordignon**: Formal analysis. **A. M. Rolim**: Formal analysis. **K. O. Araujo**: Formal analysis. **J. C. Waszak**: Formal analysis. **N. T. Brazil**: Formal analysis. **F. M. Collares**: Formal analysis. **M. Dul:** Investigation, formal analysis and writing review & editing. **R. C. Rossi**: Resources and writing review & editing. **L. S. Koester**: Conceptualization, resources, funding acquisition, writing review & editing, and supervision.

Funding: This work was supported by Conselho Nacional de Desenvolvimento Científico e Tecnológico – CNPq (406327/2025-4), Fundação de Amparo à Pesquisa do Estado do Rio Grande do Sul – FAPERGS (21/2551-0002064), and Coordenação de Aperfeiçoamento de Pessoal de Nível Superior, Finance Code 001 (CAPES).

REFERENCES

Ali, F.R., Shoaib, M.H., Ali, S.A., Yousuf, R.I., Ahmed, F.R., Siddiqui, F., Sarfaraz, S., Raja, R., 2024. Fabrication and evaluation of nanoemulsion based insulin loaded microneedles for

transdermal drug delivery. Ther. Deliv. 15, 605–617. https://doi.org/10.1080/20415990.2024.2377065

Alimardani, V., Abolmaali, S.S., Yousefi, G., Rahiminezhad, Z., Abedi, M., Tamaddon, A., Ahadian, S., 2021. Microneedle arrays combined with nanomedicine approaches for transdermal delivery of therapeutics. J. Clin. Med. 10, 181. https://doi.org/10.3390/jcm10020181

Ando, D., Miyatsuji, M., Sakoda, H., Yamamoto, E., Miyazaki, T., 2024. Mechanical characterization of dissolving microneedles: factors affecting physical strength of needles. Pharmaceutics 16. https://doi.org/10.3390/pharmaceutics16020200

Benson, H.A.E., Watkinson, A.C., 2012. Transdermal and Topical Drug Delivery: Principles and Practice, Transdermal and Topical Drug Delivery: Principles and Practice. John Wiley & Sons, Hoboken. https://doi.org/10.1002/9781118140505

Cheng, Y., Dong, Z., Liu, S., 2014. β-caryophyllene ameliorates the Alzheimer-like phenotype in APP/PS1 mice through CB2 receptor activation and the PPARγ pathway. Pharmacology 94, 1–12. https://doi.org/10.1159/000362689

Coulman, S.A., Anstey, A., Gateley, C., Morrissey, A., McLoughlin, P., Allender, C., Birchall, J.C., 2009. Microneedle mediated delivery of nanoparticles into human skin. Int. J. Pharm. 366, 190–200. https://doi.org/10.1016/j.ijpharm.2008.08.040

Danaei, M., Dehghankhold, M., Ataei, S., Hasanzadeh Davarani, F., Javanmard, R., Dokhani, A., Khorasani, S., Mozafari, M.R., 2018. Impact of particle size and polydispersity index on the clinical applications of lipidic nanocarrier systems. Pharmaceutics 10, 1–17. https://doi.org/10.3390/pharmaceutics10020057

Dul, M., Alali, M., Ameri, M., Burke, M.D., Craig, C.M., Creelman, B.P., Dick, L., Donnelly, R.F., Eakins, M.N., Frivold, C., Forster, A.H., Gilbert, P.A., Henke, S., Henry, S., Hunt, D., Lewis, H., Maibach, H.I., Mistilis, J.J., Park, J.H., Prausnitz, M.R., Robinson, D.K., Hernandez, C.A.R., Ross, C., Shin, J., Speaker, T.J., Taylor, K.M., Zehrung, D., Birchall, J.C., Jarrahian, C., Coulman, S.A., 2023. Assessing the risk of a clinically significant infection from a Microneedle Array Patch (MAP) product. J. Control. Release 361, 236–245. https://doi.org/10.1016/j.jconrel.2023.07.001

Dul, M., Alali, M., Ameri, M., Burke, M.D., Creelman, B.P., Dick, L., Donnelly, R.F., Eakins, M.N., Frivold, C., Forster, A.H., Gilbert, P.A., Henke, S., Henry, S., Hunt, D., Lewis, H., Mistilis, J.J., Park, J.H., Prausnitz, M.R., Robinson, D.K., Hernandez, C.A.R., Shin, J., Speaker, T.J., Strasinger, C., Taylor, K.M.G., Zehrung, D., Birchall, J.C., Jarrahian, C., Coulman, S.A., 2025. White paper: Understanding, informing and defining the regulatory science of microneedle-based dosage forms that are applied to the skin. J. Control. Release 378, 402–415. https://doi.org/10.1016/j.jconrel.2024.11.056

European Medicines Agency, 2022. ICH guideline Q2(R2) on validation of analytical procedures. EMA Guid. Doc. 50, 97–105.

European Medicines Agency, 2019. ICH Guideline M10 on Bioanalytical Method Validation. EMA Guid. Doc. 44, 57.

Francomano, F., Caruso, A., Barbarossa, A., Fazio, A., Torre, C. La, Ceramella, J., Mallamaci, R., Saturnino, C., Iacopetta, D., Sinicropi, M.S., 2019. β-caryophyllene: A sesquiterpene with countless biological properties. Appl. Sci. 9. https://doi.org/10.3390/app9245420

714 Gertsch, J., Leonti, M., Raduner, S., Racz, I., Chen, J.-Z., Xie, X.-Q., Altmann, K.-H., Karsak, M.,
715 Zimmer, A., 2008. Beta-caryophyllene is a dietary cannabinoid. Proc. Natl. Acad. Sci. 105,
716 9099–9104. https://doi.org/10.1073/pnas.0803601105

717 International Council for Harmonisation, 2009. ICH guideline Q8 (R2) on pharmaceutical
718 Development. Eur. Med. Agency.

719 International Council for Harmonisation, 2006. ICH Guideline Q9 on Quality Risk Management.
720 Eur. Med. Agency.

721 Johnson, A.R., Caudill, C.L., Tumbleston, J.R., Bloomquist, C.J., Moga, K.A., Ermoshkin, A.,
722 Shirvanyants, D., Mecham, S.J., Luft, J.C., De Simone, J.M., 2016. Single-step fabrication of
723 computationally designed microneedles by continuous liquid interface production. PLoS One
724 11, 1–17. https://doi.org/10.1371/journal.pone.0162518

725 Klauke, A.L., Racz, I., Pradier, B., Markert, A., Zimmer, A.M., Gertsch, J., Zimmer, A., 2014. The
726 cannabinoid CB2 receptor-selective phytocannabinoid beta-caryophyllene exerts analgesic
727 effects in mouse models of inflammatory and neuropathic pain. Eur. Neuropsychopharmacol.
728 24, 608–620. https://doi.org/10.1016/j.euroneuro.2013.10.008

729 Kreutz, T., Carneiro, S.B., Soares, K.D., Limberger, R.P., Apel, M.A., Veiga-junior, V.F., Koester,
730 L.S., 2021. Aniba canelilla (Kunth) Mez essential oil-loaded nanoemulsion: Improved stability
731 of the main constituents and in vitro antichemotactic activity. Ind. Crops Prod. 171.
732 https://doi.org/10.1016/j.indcrop.2021.113949

733 Larrañeta, E., Moore, J., Vicente-Pérez, E.M., González-Vázquez, P., Lutton, R., Woolfson, A.D.,
734 Donnelly, R.F., 2014. A proposed model membrane and test method for microneedle insertion
735 studies. Int. J. Pharm. 472, 65–73. https://doi.org/10.1016/j.ijpharm.2014.05.042

736 Li, M., Vora, L.K., Peng, K., Sabri, A.H.B., Qin, N., Abbate, M., Paredes, A.J., Mccarthy, H.O.,
737 Donnelly, R.F., 2024. Novel nano-in-micro fabrication technique of diclofenac nanoparticles
738 loaded microneedle patches for localised and systemic drug delivery. Biomater. Adv. 161,
739 213889. https://doi.org/10.1016/j.bioadv.2024.213889

740 Lucca, L.G., de Matos, S.P., Weimer, P., Teixeira, H.F., Koester, L.S., 2020. Improved skin
741 delivery and validation of novel stability-indicating HPLC method for ketoprofen
742 nanoemulsion. Arab. J. Chem. 13, 4505–4511. https://doi.org/10.1016/j.arabjc.2019.09.005

743 Makvandi, P., Kirkby, M., Hutton, A.R.J., Shabani, M., Yiu, C.K.Y., Baghbantaraghdari, Z.,
744 Jamaledin, R., Carlotti, M., Mazzolai, B., Mattoli, V., Donnelly, R.F., 2021. Engineering
745 microneedle patches for improved penetration: analysis, skin models and factors affecting
746 needle insertion, Nano-Micro Letters. Springer Singapore. https://doi.org/10.1007/s40820-021-
747 00611-9

748 MAP RWG, 2024. Microneedle Array Patch Regulatory Working Group [WWW Document]. URL
749 https://www.microneedleregulatory.org/ (accessed 7.1.24).

750 McAlister, E., Kearney, M.C., Martin, E.L., Donnelly, R.F., 2021. From the laboratory to the end-
751 user: a primary packaging study for microneedle patches containing amoxicillin sodium. Drug
752 Deliv. Transl. Res. 11, 2169–2185. https://doi.org/10.1007/s13346-020-00883-5

753 Meza, A., Lehmann, C., 2018. Betacaryophyllene – A phytocannabinoid as potential therapeutic
754 modality for human sepsis? Med. Hypotheses 110, 68–70.
755 https://doi.org/10.1016/j.mehy.2017.10.025

Mir, M., Permana, A.D., Ahmed, N., Khan, G.M., Rehman, A. ur, Donnelly, R.F., 2020. Enhancement in site-specific delivery of carvacrol for potential treatment of infected wounds using infection responsive nanoparticles loaded into dissolving microneedles: A proof of concept study. Eur. J. Pharm. Biopharm. 147, 57–68. https://doi.org/10.1016/j.ejpb.2019.12.008

Moawad, F., Pouliot, R., Brambilla, D., 2025. Dissolving microneedles in transdermal drug delivery: A critical analysis of limitations and translation challenges. J. Control. Release 383, 113794. https://doi.org/10.1016/j.jconrel.2025.113794

Mödinger, Y., Knaub, K., Dharsono, T., Wacker, R., Meyrat, R., Land, M.H., Petraglia, A.L., Schön, C., 2022. Enhanced oral bioavailability of β-Caryophyllene in healthy subjects using the VESIsorb® formulation technology, a novel self-emulsifying drug delivery system (SEDDS). Molecules 27. https://doi.org/10.3390/molecules27092860

Nasiri, M.I., Vora, L.K., Ershaid, J.A., Peng, K., Tekko, I.A., Donnelly, R.F., 2022. Nanoemulsion-based dissolving microneedle arrays for enhanced intradermal and transdermal delivery. Drug Deliv. Transl. Res. 12, 881–896. https://doi.org/10.1007/s13346-021-01107-0

National Center for Biotechnology Information, 2019. PubChem CID: 5281515 [WWW Document].

NCBI, N.C. for B.I., 2022. Caryophyllene [WWW Document]. Natl. Libr. Med. URL https://pubchem.ncbi.nlm.nih.gov/compound/5281515

OCDE 428, 2004. OECD - GUIDELINE FOR THE TESTING OF CHEMICALS: Skin Absorption: in vitro Method. Test 1–8. https://doi.org/10.1787/9789264071087-en

Olatunji, O., Das, D.B., Garland, M.L., Belaid, L., Donnelly, R.F., 2013. Influence of array interspacing on the force required for successful microneedle skin penetration: theoretical and practical approaches. J. Pharm. Sci. 120, 1209–1221. https://doi.org/10.1002/jps

Permana, A.D., Anjani, Q.K., Sartini, Utomo, E., Volpe-Zanutto, F., Paredes, A.J., Evary, Y.M., Mardikasari, S.A., Pratama, M.R., Tuany, I.N., Donnelly, R.F., 2021. Selective delivery of silver nanoparticles for improved treatment of biofilm skin infection using bacteria-responsive microparticles loaded into dissolving microneedles. Mater. Sci. Eng. C 120, 111786. https://doi.org/10.1016/j.msec.2020.111786

Permana, A.D., McCrudden, M.T.C., Donnelly, R.F., 2019. Enhanced intradermal delivery of nanosuspensions of antifilariasis drugs using dissolving microneedles: A proof of concept study. Pharmaceutics 11, 1–22. https://doi.org/10.3390/pharmaceutics11070346

Permana, A.D., Mir, M., Utomo, E., Donnelly, R.F., 2020. Bacterially sensitive nanoparticle-based dissolving microneedles of doxycycline for enhanced treatment of bacterial biofilm skin infection: A proof of concept study. Int. J. Pharm. X 2, 100047. https://doi.org/10.1016/j.ijpx.2020.100047

Peterle, J.P., Bidone, J., Lucca, L.G., Araújo, G. de M.S., Falkembach, M.C., Marques, M. da S., Horn, A.P., Dos Santos, M.K., Veiga Jr, V.F., Limberger, Renata Pereira Teixeira, H.F., Dora, C.L., Koester, L.S., 2020. Healing activity of hydrogel containing nanoemulsified β-caryophyllene. Eur. J. Pharm. Sci. 148. https://doi.org/10.1016/j.ejps.2020.105318

Politis, S.N., Colombo, P., Colombo, G., Rekkas, D.M., Politis, S.N., Colombo, P., Colombo, G., Rekkas, D.M., 2017. Design of experiments (DoE) in pharmaceutical development. Drug Dev.

Ind. Pharm. 43, 889–991. https://doi.org/10.1080/03639045.2017.1291672

Rai, V.K., Mishra, N., Yadav, K.S., Yadav, N.P., 2018. Nanoemulsion as pharmaceutical carrier for dermal and transdermal drug delivery: Formulation development, stability issues, basic considerations and applications. J. Control. Release 270, 203–225. https://doi.org/10.1016/j.jconrel.2017.11.049

Sharma, C., Al Kaabi, J.M., Nurulain, S.M., Goyal, S.N., Kamal, M.A., Ojha, S., 2016. Polypharmacological properties and therapeutic potential of β-caryophyllene: a dietary phytocannabinoid of pharmaceutical promise. Curr. Pharm. Des. 22, 3237–3264. https://doi.org/10.2174/1381612822666160311115226

Sheskey, P.J., Hancock, B.C., Moss, G.P., Goldfarb, D.J., 2020. Handbook of Pharmaceutical Excipients, 9th ed. Pharmaceutical Press, London.

Simões, A., Veiga, F., Vitorino, C., 2024. Question-based review for pharmaceutical development: an enhanced quality approach. Eur. J. Pharm. Biopharm. 195. https://doi.org/10.1016/j.ejpb.2023.114174

Singh, Y., Gopal, J., Raval, K., Ali, F., Chaurasia, M., Jain, N.K., Chourasia, M.K., 2017. Nanoemulsion: Concepts, development and applications in drug delivery. J. Control. Release 252, 28–49. https://doi.org/10.1016/j.jconrel.2017.03.008

Srivastava, P.K., Thakkar, H.P., 2021. QbD-driven development of dissolving microneedle patch loaded with ultradeformable liposomes encapsulated Noopept: Exploring a patient friendly, once-daily option to manage dementia. Eur. J. Pharm. Sci. 164, 105909. https://doi.org/10.1016/j.ejps.2021.105909

Volpe-Zanutto, F., Ferreira, L.T., Permana, A.D., Kirkby, M., Paredes, A.J., Vora, L.K., P. Bonfanti, A., Charlie-Silva, I., Raposo, C., Figueiredo, M.C., Sousa, I.M.O., Brisibe, A., Costa, F.T.M., Donnelly, R.F., Foglio, M.A., 2021. Artemether and lumefantrine dissolving microneedle patches with improved pharmacokinetic performance and antimalarial efficacy in mice infected with Plasmodium yoelii. J. Control. Release 333, 298–315. https://doi.org/10.1016/j.jconrel.2021.03.036

Weimer, P., Kirsten, C.N., de Araújo Lock, G., Nunes, K.A.A., Rossi, R.C., Koester, L.S., 2023. Co-delivery of beta-caryophyllene and indomethacin in the oily core of nanoemulsions potentiates the anti-inflammatory effect in LPS-stimulated macrophage model. Eur. J. Pharm. Biopharm. 191, 114–123. https://doi.org/10.1016/j.ejpb.2023.08.020

Weimer, P., Kreutz, T., Limberger, R.P., Rossi, R.C., de Lima, Á.A.N., Veiga, V.F., de Araújo, B.V., Koester, L.S., 2022. Correlation between the skin permeation profile of the synthetic sesquiterpene compounds, beta-Caryophyllene and caryophyllene oxide, and the antiedematogenic activity by topical application of nanoemulgels. Biomolecules 12. https://doi.org/10.3390/biom12081102

Weimer, P., Rossi, R.C., Koester, L.S., 2021. Dissolving microneedles developed in association with nanosystems: A scoping review on the quality parameters of these emerging systems for drug or protein transdermal delivery. Pharmaceutics 13. https://doi.org/10.3390/pharmaceutics13101601

FIGURE LEGENDS

Figure 1 – Pareto chart plots of 2^4 Full Factorial Design for **(A)** β-caryophyllene content and **(B)** compression force; The horizontal bars beyond the dotted line represent statistically significant input factors by linear or interaction terms ($p < 0.05$). Main effects plots of 2^4 Full Factorial Design for **(C)** β-caryophyllene content and **(D)** compression force.

Figure 2 - Contour plots of Box–Behnken Design showing effects on β-caryophyllene content: **(A)** β-caryophyllene:polymer ratio (car:polymer ratio) versus polymer solids (% w/w); **(B)** PVP:PVA ratio versus polymer solids (% w/w); **(C)** β-caryophyllene:polymer ratio (car:polymer ratio) versus PVP:PVA ratio. Contour plot of optimized condition **(D)**. The white region of the graph indicates the design space in which the β-caryophyllene content can be obtained above 90% with PVP:PVA ratio fixed at 1.54.

Figure 3 - Macroscopic appearance of the dissolving microneedles integrated with β-caryophyllene nanoemulsion after optimization by Box–Behnken Design **(A)**. Digital microscopies of **(B)** formulation optimized by Box–Behnken Design, **(C)** perforated Parafilm® layers after *in vitro* skin insertion test (32.0 N application force), **(D)** porcine ear skin before and after perforation with microneedle array.

Figure 4 – Results of optical coherence tomography **(A)** 2D cross-sectional scans over time. **(B)** Graph showing area reduction of the needle inserted into the skin over time.

Figure 5 - Scanning electron microscopy of **(A)** blank microneedles, needles composed of PVP 40 kDa and PVA 9-10 kDa in concentration equivalent to the optimized formulation, **(B)** formulation optimized by Box–Behnken Design, needles composed of PVP 40 kDa and PVA 9-10 kDa in association with nanoemulsion β-caryophyllene. The green markings indicate the dimensions of the needles generated at 10.0 kV and 150× magnification (EVO MA10). X-ray microcomputed tomography (XμCT) of formulation optimized by Box–Behnken Design **(C, D)**.

Figure 6 - Data from a preliminary stability study of the optimized microneedle array stored in aluminum sachets (25 °C ± 5 °C, 40% ± 10% RH). **(A)** β-caryophyllene content, **(B)** compression force, **(C)** *in vitro* skin insertion efficiency, **(D)** variation mass of the arrays. *Statistical difference in relation to T1 by two-way ANOVA followed by Tukey's test ($p < 0.05$).

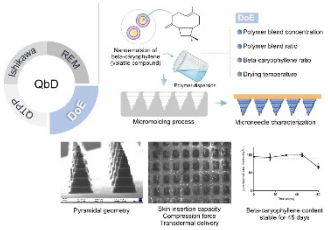

HIGHLIGHTS

- QbD-driven development of an integrated dissolvable MN system with nanoemulsion
- Understanding the impact of formulation variables on content maintenance and CQAs
- Proof of the viability of β-caryophyllene delivery through polymeric MN
- Promotion of transdermal release with association of nanoemulsion in polymeric MN
- Maintaining the content of the lipophilic and volatile compound in MN for 45 days

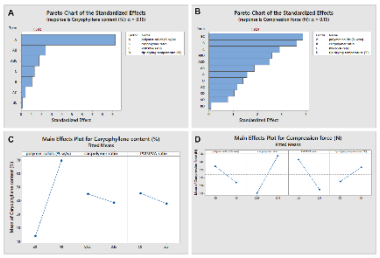

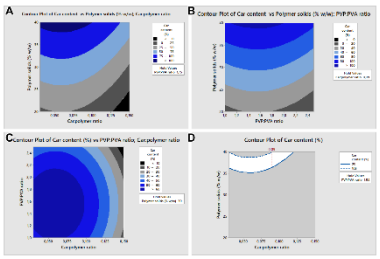

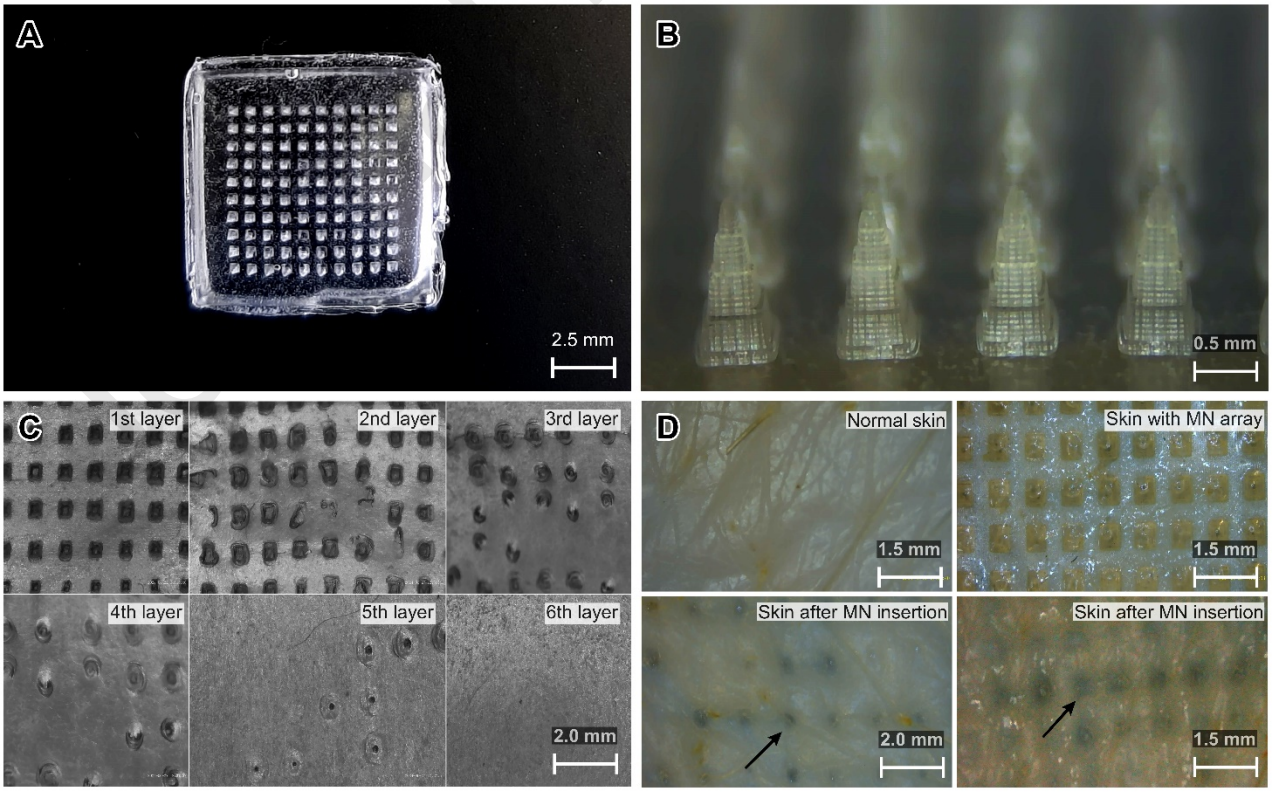

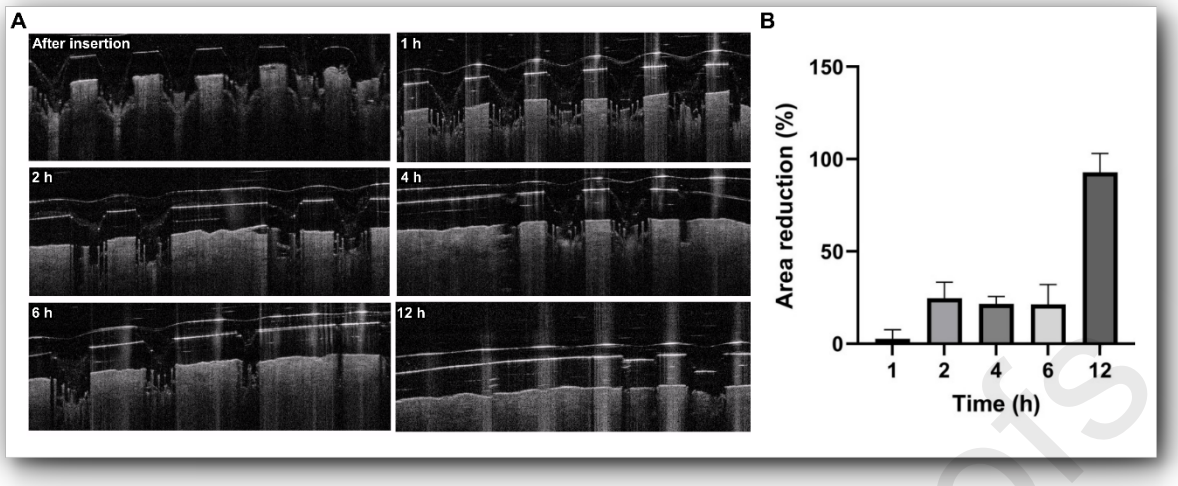

884

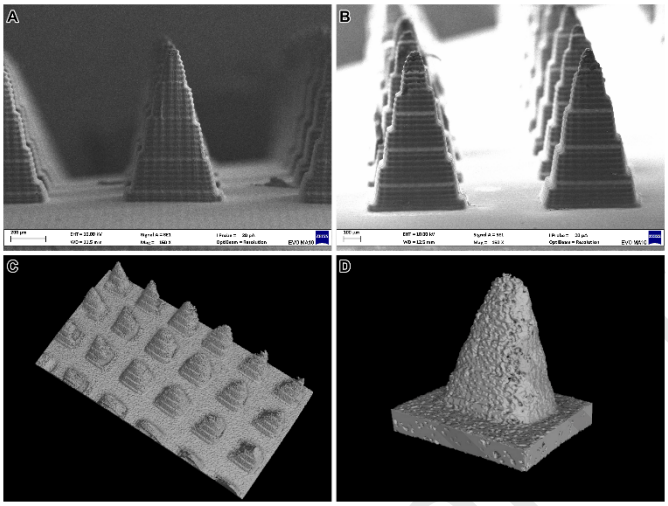

885

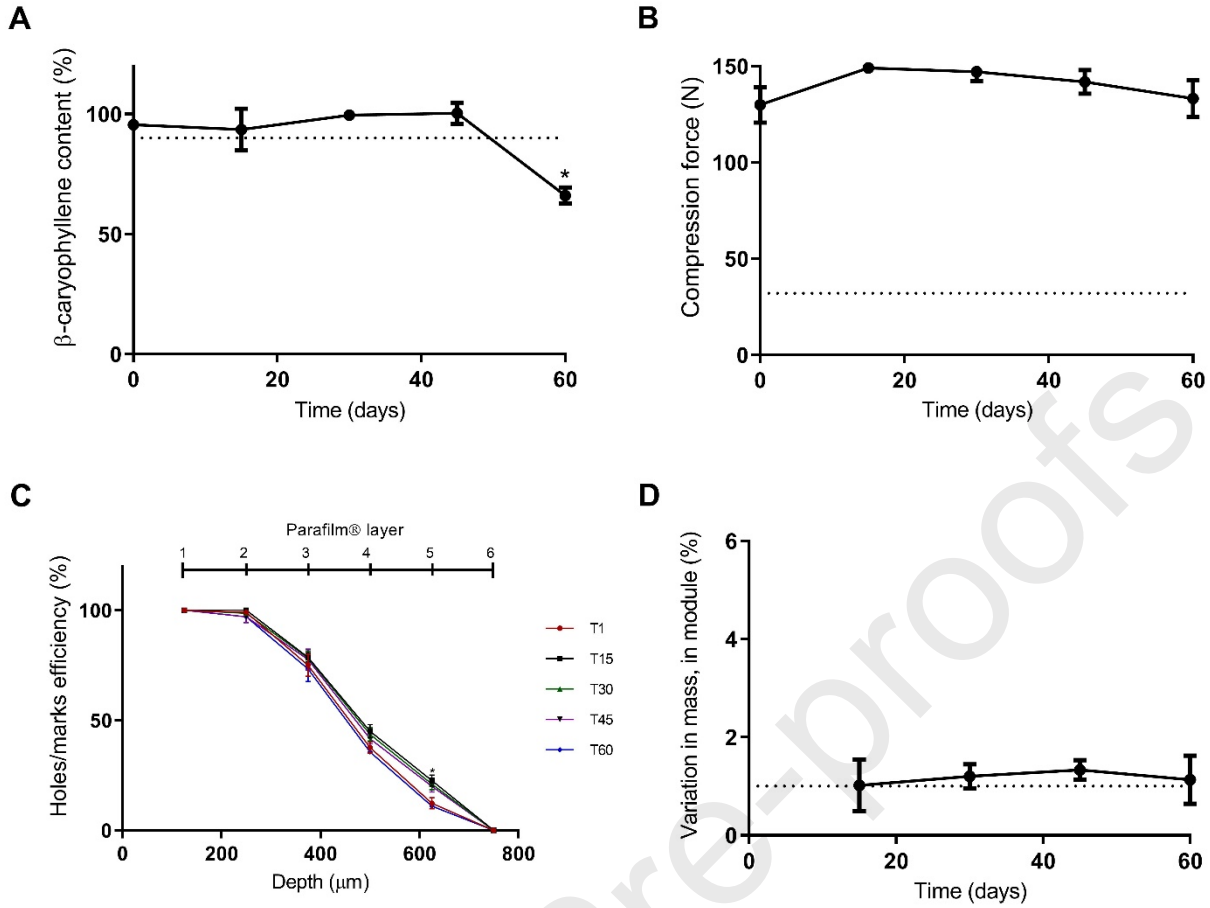

886